Article

Modi-2 a vaccine stimulating CD4 responses to homocitrullinated self epitopes as therapy for solid cancers

Check for updates

Abdullah A. Al-Omari [1], Katherine W. Cook [1], Peter Symonds[1], Anne Skinner[1], Alissa Wright[1], Yaling Zhu[2], Vincent L. Coble[2], Omar J. Mohammed[1], Ruhul H. Choudhury[1], Nazim Uddin [1], Priscilla Ranglani[1], Adrian Parry[1], Sally E. Adams[1], Geoffrey M. Lynn[2], Lindy G. Durrant[1] ✉ & Victoria A. Brentville[1]

Stresses within the tumour microenvironment can mediate post-translational modifications of self-proteins. Homocitrullination is the conversion of lysine to homocitrulline which generates neoepitopes and bypasses self-tolerance. In this study a vaccine targeting homocitrullinated antigens was assessed for stimulation of anti-tumour immunity. Peptides that bind HLA are often hydrophobic which can complicate large scale manufacture and solubility. Here we demonstrate the self-assembling nanoparticle technology (SNAPvax™) to co-deliver four homocitrullinated peptides and adjuvant in nanoparticles of a precise size and composition as a vaccine ("Modi-2") that is optimized for manufacturing ease and T cell induction. Strong T cell responses and anti-tumour immunity in mouse tumour models was stimulated against against B16 melanoma ($p = 0.0113$), CT26 colorectal cancer ($p < 0.0001$) and 4T1 breast cancer ($p = 0.0090$). We demonstrate that human lung, colorectal, breast and prostate tumours express the Modi-2 target antigens and propose the Modi-2 vaccine has potential for translation into clinic in several cancer indications.

The cellular stress of the tumour microenvironment (TME) can induce post-translational modifications (PTMs) of proteins that can appear foreign to the immune and be recognized as antigens[1]. One such PTM is homo-citrullination or carbamylation which is the conversion of lysine residues to homocitrulline. This results in the conversion of a positively charged amino acid lysine into a neutral amino acid homocitrulline and can result in altered MHC binding properties[2]. The conversion of lysine to homocitrulline is driven by the accumulation of cyanate[3,4], which under inflammatory conditions, is driven by the myeloperoxidase (MPO) enzyme. We have previously demonstrated a role for MPO-producing tumour-associated myeloid derived suppressor cells (MDSCs) in MPO production which in combination with tumour produced H_2O_2 leads to homocitrullination within the tumour microenvironment[5].

Mutational neo-antigens that also are not subject to immune tolerance are linked to the success of checkpoint blockade therapies in several indications and are showing promising results as targets for vaccination[6–8]. However, many cancers do not possess a high mutational burden and show limited efficacy to checkpoint blockade therapies. Stress-related PTMs alter proteolytic cleavage and can generate neoantigens or neoepitopes which

evade self-tolerance[9,10]. In this scenario these cancers may benefit from de novo induction of PTM specific T cell responses via vaccination. Vaccination targeting homocitrullinated peptides derived from self-antigens has been shown to stimulate Th1 mediated immune responses in mouse models and mediate tumour therapy[5,11]. Many cancer vaccines have been focussed on the stimulation of CD8 T cell responses and their role in tumour therapy rather than CD4 responses although the important role of CD4 T cells is now becoming more apparent[12,13]. CD4 T cells play an important role in cancer therapy and can either directly mediate the destruction of established tumours[14,15] and/or indirectly by their interaction with APCs which induces the release of interferons that then upregulate MHC-I/II and stimulate the release of pro-inflammatory chemokines to promote further immune infiltration[13,16].

The efficacy of a peptide vaccine is also enhanced if combined with a costimulatory adjuvant. Toll-like receptor (TLR) ligand stimulation in combination with vaccination has been shown to increase vaccine efficacy, especially for cancer therapy[17]. Despite many early phase trials with new TLR ligand adjuvants only a few have been approved for use in humans. We and others have demonstrated in preclinical models the benefit of

[1]Scancell Ltd; Bellhouse Building, Sanders Road, Oxford Science Park, Oxford, OX4 4GD, UK. [2]Barinthus Biotherapeutics North America, Inc; 20400 Century Blvd, Suite 210, Germantown, MD, 20874, USA. ✉e-mail: lindydurrant@scancell.co.uk

utmb Health
Sealy Institute for Vaccine Sciences

combining a peptide vaccine with a TLR ligand adjuvant to promote CD8 and CD4 T cell responses[18-21]. TLR ligands that stimulate strong Th1 immunity are often hydrophobic in nature and combined with hydrophobic nature of MHC binding peptides can lead to challenges for large scale manufacture and sterile filtration. The SNAPvax technology which enables formulation of hydrophobic MHC binding peptides with TLR 7/8 ligand that self assembles into nanoparticles has demonstrated superior immunogenicity and stimulation of CD8 T cell responses. Antigen delivered in this particulate form not only persisted longer at the dosing site but was also associated with uptake by APCs in draining lymph nodes[21,22]. In mouse models, no evidence of systemic localisation is noted unless delivered via an intravenous route[23].

Here we demonstrate the combination of four homocitrullinated peptides from self-antigens, vimentin, aldolase A, Binding Immunoglobulin Protein (BiP) which is also known as "GRP78" and cytokeratin 8, combined with TLR ligand adjuvant as a peptide vaccine (Modi-2) stimulates strong Th1 mediated anti-tumour responses in mouse models. We further show that the formulation characteristics of the Modi-2 vaccine can be improved using SNAPvax technology wherein each of the homocitrullinated peptides were synthesized as amphiphiles linked to TLR ligand and self-assemble into nanoparticles of precise size and composition co-delivering the four peptides and TLR ligand for induction of CD4 T cell responses and tumour therapy. Finally, we highlight the expression of the self-antigens and MPO in solid tumours and association with prognosis and propose using the SNAPvax technology for targeting of homocitrullinated self-antigens via vaccination for solid tumour therapy.

Results

Responses to homocitrullinated peptides can be stimulated in mice and are CD4 mediated

Proteins containing homocitrulline modifications are known to be immunogenic. We have previously shown that homocitrullinated (Hcit) peptides derived from aldolase A (Aldo), immunoglobulin heavy chain-binding protein (BiP), cytokeratin 8 (Cyk8) and vimentin (Vim) can stimulate CD4 T cell responses through multiple MHCII alleles in standard and HLA transgenic mice including HLA-HHDII/DR1, HLA-HHDII/DP4, HLA-DR4 and Balb/c mice. We have also observed that among several peptides screened, Aldo74-93[Hcit], BiP562-579[Hcit], Cyk8 371-388[Hcit] and Vim116-135[Hcit] peptides induced T cell responses in the different mouse strains mentioned above[5,11]. These epitopes are homologous in humans and mice. In this study we first aimed to confirm whether vaccination of Aldo74-93[Hcit], BiP562-579[Hcit], Cyk8 371-388[Hcit] and Vim116-135[Hcit] in combination (known as Modi-2) mixed with CpG and MPLA adjuvants would induce T cell responses in different mice strains. A schematic of the immunisation regime is shown in Fig. 1A. HLA-HHDII/DP4 and Balb/c mice immunised with the Modi-2 peptide combination were screened for peptide specific responses in IFNγ ELISpot assay. This screening showed significant responses to Aldo74-93[Hcit] ($p = 0.0005$), Bip562-579[Hcit] ($p < 0.0001$) and Vim116-135[Hcit] ($p = 0.0472$) in HLA-HHDII-DP4 mice (Fig. 1B). However no immune responses to Cyk8 371-388[Hcit] were observed in HLA-HHDII-DP4 mice. Balb/c mice induced significant immune responses to Aldo74-93[Hcit] ($p = 0.0042$), Cyk8 371-388[Hcit] ($p = 0.0021$) and Vim116-135[Hcit] ($p = 0.0014$). However, no immune responses to Bip562-579[Hcit] were identified in Balb/c mice (Fig. 1E). Mice immunised with the CpG and MPLA adjuvants alone, irrelevant peptide in CpG and MPLA or naïve mice failed to show any reactivity to the Hcit peptides (Supplementary Fig. 1).

To confirm whether responses to the Modi-2 peptides were modification specific without cross reactivity to the wild type (wt) peptides, responses to Aldo74-93[wt], Bip562-579[wt], Cyk8 371-388[wt] and Vim116-135[wt] peptides were assessed in HLA-HHDII/DP4 and Balb/c mice. IFNγ responses to Aldo74-93[Hcit], Bip562-579[Hcit] and Vim116-135[Hcit] were significantly higher than the responses to Aldo74-93[wt], Bip562-579[wt] and Vim116-135[wt], $p < 0.0001$, $p < 0.0001$ and $p = 0.0286$ respectively, showing minimal cross reactivity to the wt peptides in HLA-HHDII/DP4 mice (Fig. 1C). Similar findings were observed in Balb/c mice where IFNγ

responses to Aldo74-93[Hcit], Cyk8 371-388[Hcit] and Vim116-135[Hcit] were significantly higher than the responses to Aldo74-93[wt], Cyk8 371-388[wt] and Vim116-135[wt], $p = 0.0030$, $p = 0.0130$ and $p = 0.0011$ respectively, with minimal cross reactivity to the wt peptides (Fig. 1F). Vaccination with Modi-2 peptides, that are 18–20 amino acids in length, may stimulate both CD4 and CD8 IFNγ responses. Therefore, we further investigated whether responses to the combination of Modi-2 peptides were mediated by CD4 or CD8 T cells. In HLA-HHDII/DP4 mice, blocking CD4 T cells in the ELISpot assay significantly reduced IFNγ responses to Aldo74-93[Hcit] ($p = 0.0322$) and Bip562-579[Hcit] ($p = 0.0466$) but blocking CD8 T cells had no significant effect on responses to those peptides (Fig. 1D). Responses to Vim116-135[Hcit] were reduced by the anti-CD4 blocking antibody but this did not reach significance and were also partially blocked by the anti-CD8 blocking antibody in HLA-HHDII/DP4 mice (Fig. 1D). In Balb/c mice, IFNγ responses to Aldo74-93[Hcit], Cyk8 371-388[Hcit] and Vim116-135[Hcit] were significantly reduced after blocking CD4 T cells, while blocking CD8 T cells had no significant impact on the IFNγ responses (Fig. 1G). Example ELISpot images are shown in Fig. 1H.

Together these results confirm that vaccination with the Modi-2 peptides can stimulate IFNγ responses in transgenic mice expressing human HLA-DP4 and Balb/c mice which express murine H-2d haplotype. However, responses vary between different mice strains. These results also support previous data[5,10] and confirm that responses to the Modi-2 peptides are homocitrulline-specific and mediated by CD4 T cells.

Modi-2 peptides can be formulated with SNAPvax technology to enable codelivery with immunomodulatory adjuvant and facilitate manufacturing

Peptide based vaccines require delivery with an immunostimulatory adjuvant that enhances the magnitude and quality of immune responses. In addition, manufacturing peptide-based vaccines provides many challenges. Most immunogenic peptides are hydrophobic in nature and therefore they have high aggregation potential and low solubility in aqueous or organic solvents. These factors make peptide-based vaccines difficult to manufacture to clinical GMP scale. The mixture of Modi-2 peptides with CpG/MPLA adjuvant does indeed show very large particle sizes with an aggregation of particulate matter which is highly polydisperse (Fig. 2A and Supplementary Table 6). Similar moderate size particles are seen for the Modi-2 peptides mixed with TLR7/8 adjuvant (Supplementary Fig. 2 and Supplementary Table 6). These large particle sizes result in significant material loss upon sterile filtration through a 0.2 μm filter (Supplementary Table 7).

Here we describe the use of the SNAPvax technology (Barinthus Biotherapeutics plc) which incorporates peptide antigens in amphiphiles linked to combined TLR-7 & -8 (TLR-7/8) ligands that self-assemble into ~20 nm nanoparticle micelles (Fig. 2B)[21]. Covalently linking peptide antigens and TLR-7/8 ligands ensures codelivery to the same APC, while use of amphiphiles that self-assemble to uniformly small nanoparticles (~ 20 nm) well below the size cut-off for sterile filters (~ 200 nm) improves manufacturability by providing both improved solubility in aqueous buffers and compatibility with sterile filtration. We first assessed the impact of the buffer on the size of nanoparticles formed with the Modi-2 SNAPvax formulations. Modi-2 SNAPvax was formulated in different aqueous buffers including PBS, Histidine (His) and Tris that enables sterile filtration through a 0.2 μm filter. The DLS analysis showed that the nanoparticle size of Modi-2 SNAPvax in histidine formulation was 12.6 nm ± 0.9 SD, whereas it was 14.3 nm ± 0.2 SD and 15.5 nm ± 0.1 SD in Tris and PBS formulation, respectively (Fig. 2C) with low polydispersity index values (Supplementary Table 6).Transmission electron microscopy analysis confirmed the spherical shape and similar size of the particles compared to DLS measurement. Example transmission electron micrograph images of nanoparticle formulations are shown in Fig. 2D. Zeta potential at respective formulation pH is shown in Supplementary Table 6. Modi-2 SNAPvax in histidine, with a zeta potential value of +35 mV, indicates that the particles are not prone to forming aggregates; hence, the formulation should remain stable.
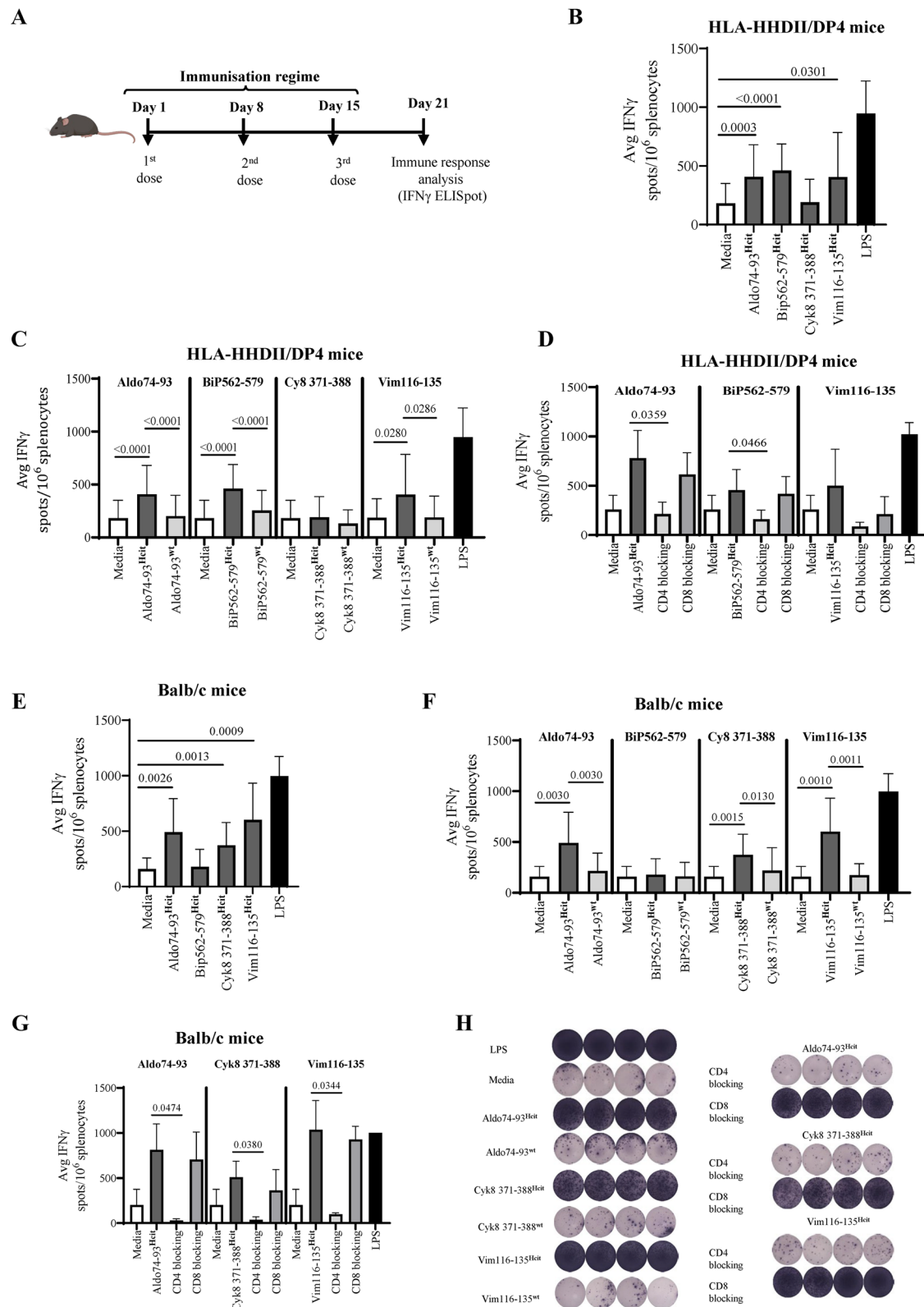
Fig. 1 | Modi-2 peptides elicit Hcit specific CD4 mediated responses in mice.
Schematic of immunisation regime (**A**). T cell responses to the Modi-2 peptides and counterpart wild type peptides in HLA-HHDII/DP4 (**B–D**) and Balb/c mice (**E–H**). Mice were vaccinated with three doses of homocitrullinated peptides mixed with the adjuvants CpG and MPLA and responses assessed against Hcit peptides (**B**, **E**), Hcit and wt peptides (**C**, **F**) or Hcit peptides in presence of CD4 or CD8 blocking antibodies (**D**, **G**) by IFNγ ELISpot assay. Representative ELISpot images (**H**). $n \geq 3$ in each study and data is collated from at least two independent studies. Mean, standard deviations and significant p values are shown. Image in (**A**) created with BioRender.com.
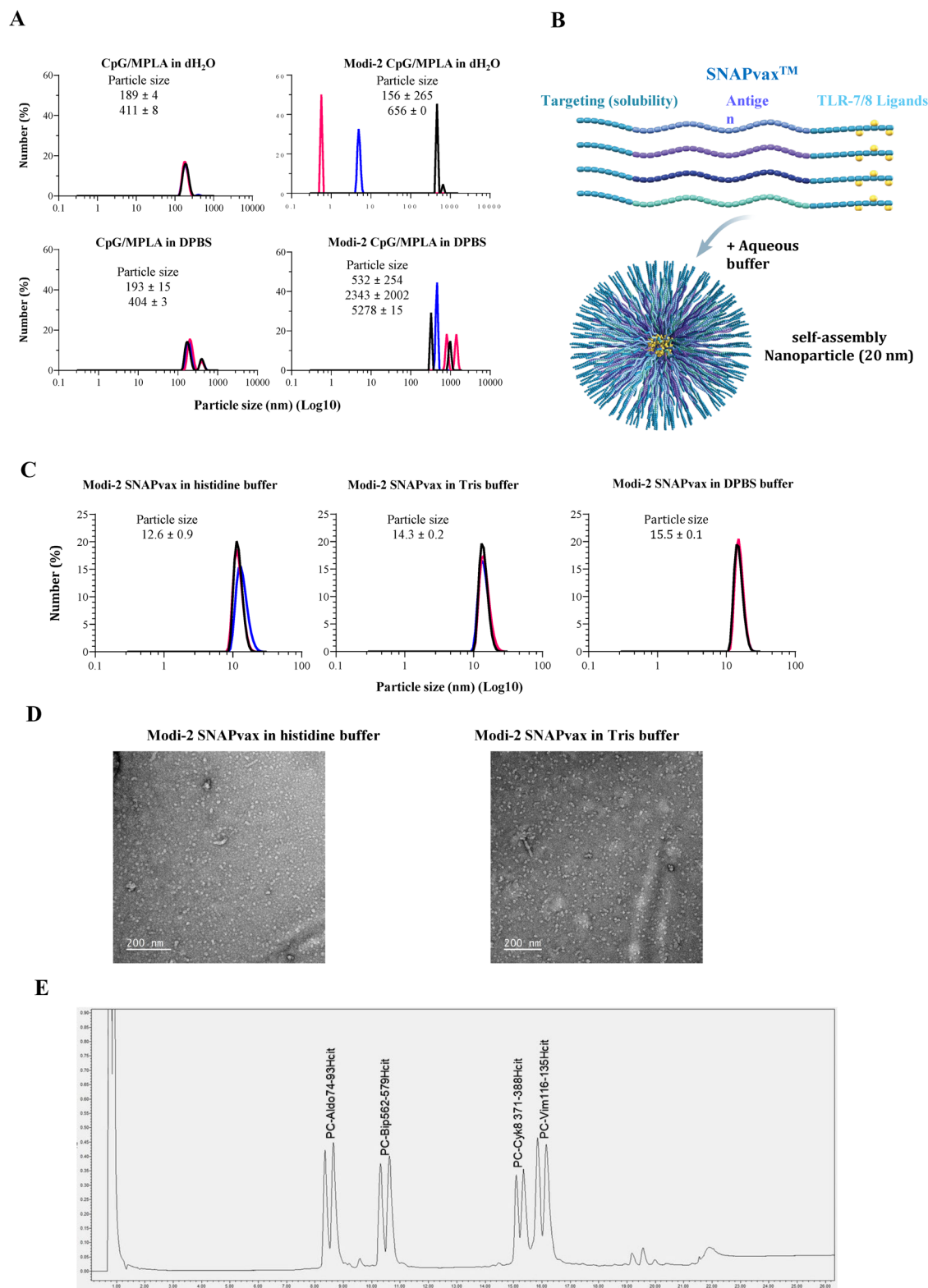
Fig. 2 | Formulation of Modi-2 peptides with SNAPvax technology. A DLS histograms showing the size of particles of Modi-2 peptides in CpG/MPLA or TLR7/8 formulation. Each colour represents a different repeat measurement. **B** A schematic figure of the SNAPvax (Self-assembling Nanoparticles based on Amphiphilic Peptides) platform. **C** DLS histograms showing the size of nanoparticles of Modi-2 SNAPvax formulations in different buffers. The particle size is shown in nanometer[22] ± standard deviation (SD). Each colour represents a different repeat measurement. At least 3 replicate assays were performed. **D** Transmission electron micrograph images of Modi-2 SNAPvax formulations in Histidine or Tris buffers. **E** UPLC-PDA chromatogram showing distinct peaks for each of Modi-2 peptides in the SNAPvax formulation. Images in (**B**) from Barinthus Biotherapeutics.
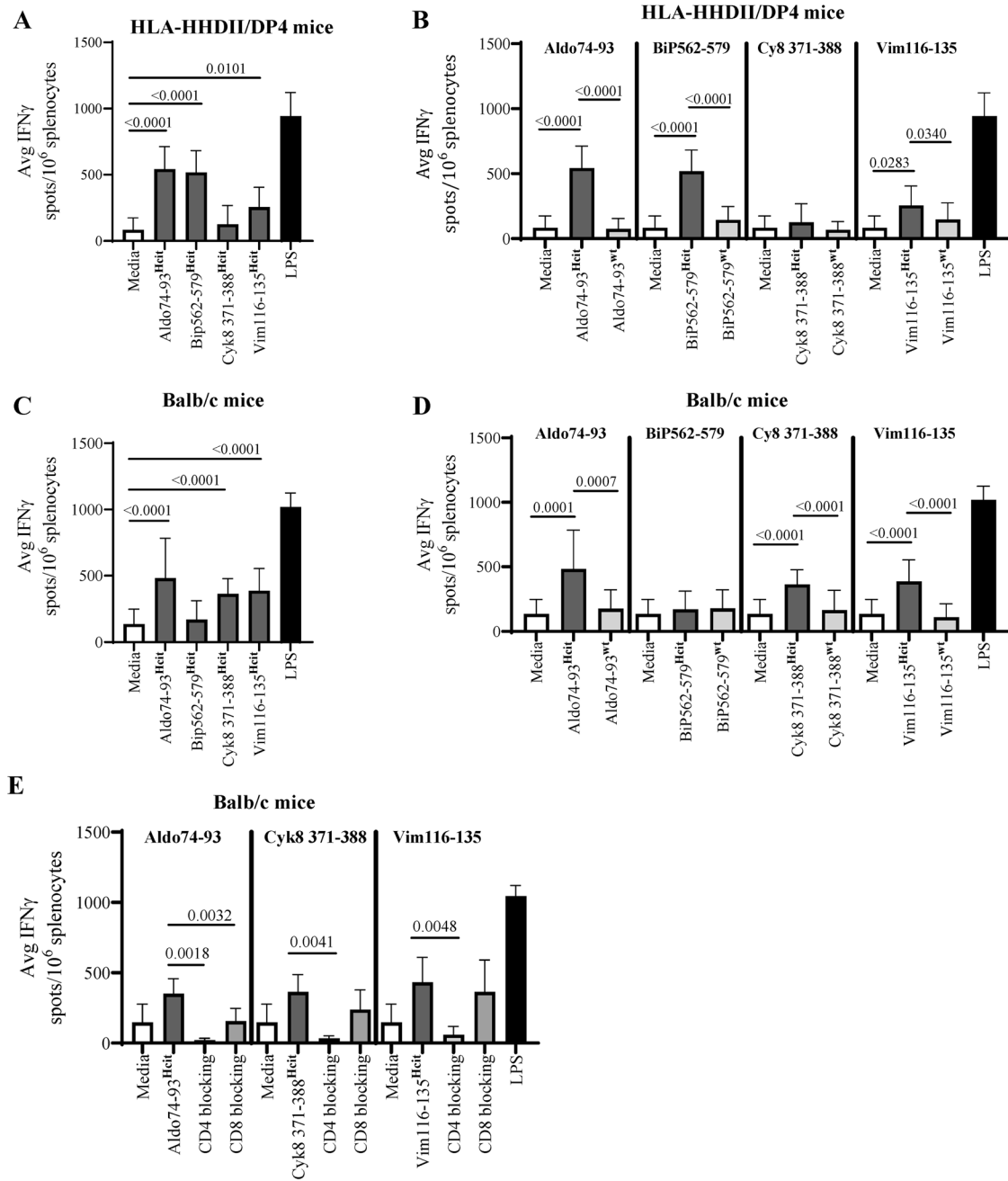
Fig. 3 | Modi-2 SNAPvax stimulates Hcit specific CD4 responses. T cell responses to the Modi- 2 homocitrullinated and matched wild type peptides in HLA-HHDII/DP4 (**A**, **B**) and Balb/c mice (**B–E**). Mice were vaccinated with three doses of homocitrullinated peptides conjugated to SNAPvax and responses assessed against Hcit peptides (**A**, **C**), Hcit and wt peptides (**C**, **D**) or Hcit peptides in presence of CD4 or CD8 blocking antibodies (**E**). $n \geq 3$ in each study and data is collated from at least two independent studies. Mean, standard deviations and significant *p*-values are shown.

In addition, minimal material loss is reported upon sterile filtration from the nanoparticle formulations (Supplementary Table 7). As Modi-2 SNAPvax were formulated as "mosaic formulation" where each nanoparticle contains all four homocitrullinated peptide antigens, we used UPLC-PDAMS analysis to confirm that the four Modi-2 peptides with distinct peaks were detected (Fig. 2E). These results confirm that Modi-2 SNAPvax forms nanoparticles with similar size and mosaic composition of the four homocitrullinated peptides when formulated in different aqueous buffers. To further assess the stability of the Modi-2 SNAPvax formulations particle size was assessed over time with storage at −20 °C (Supplementary Figure 3) and with repeat freeze thaw cycles (Supplementary Fig. 4) and shown to retain initial particle size characteristics with multiple freeze thaws and over a 12-month period stored at −20 °C.

Modi-2 vaccine can stimulate efficient immune responses as a SNAPvax formulation

Modi-2 SNAPvax formulations were assessed for the capacity to induce antigen-specific T cell responses in mice as confirmed by IFNγ ELISpot analysis following vaccination. HLA-HHDII/DP4 and Balb/c mice were vaccinated with three doses of Modi-2 SNAPvax formulations and responses to homocitrullinated and wild type peptides were screened ex vivo. This screening showed significant responses to Aldo74-93^{Hcit} ($p < 0.0001$), Bip562-579^{Hcit} ($p < 0.0001$) and Vim116-135^{Hcit} ($p = 0.0101$) in HLA-HHDII/DP4 mice (Fig. 3A). Balb/c mice showed significant responses to Aldo74-93^{Hcit} ($p < 0.0001$), Cyk8 371-388^{Hcit} ($p < 0.0001$) and Vim116-135^{Hcit} ($p < 0.0001$) (Fig. 3C). Mice immunised with TLR7/8 adjuvant only or an irrelevant peptide SNAPvax formulation demonstrate no Hcit peptide

specific responses (Supplementary Fig. 5) This data is consistent with the responses seen from the peptides mixed with CpG and MPLA adjuvants. Direct comparisons of SNAPvax formulation with peptide mixed with CpG and MPLA or TLR7/8 adjuvants is shown in Supplementary Fig. 5. Since Modi-2 SNAPvax can be formulated with similar particle size in different buffers the formulations of Modi-2 SNAPvax were assessed in PBS, histidine or tris containing buffers for immunogenicity and all stimulated similar immune responses (Supplementary Fig. 6).

Responses to Modi-2 SNAPvax formulations were also homocitrulline-specific showing no cross reaction to the wild-type peptides. IFNγ responses to Aldo74-93[Hcit], Bip562-579[Hcit] and Vim116-135[Hcit] were significantly higher than the responses to Aldo74-93[wt], Bip562-579[wt] and Vim116-135[wt], $p < 0.0001$, $p < 0.0001$ and $p = 0.0283$ respectively, confirming minimal cross reactivity to the wt peptides in HLA-HHDII/DP4 mice (Fig. 3B). Similar findings were seen in Balb/c mice where IFNγ responses to Aldo74-93[Hcit], Cyk8 371-388[Hcit] and Vim116-135[Hcit] were significantly higher than the responses to Aldo74-93[wt], Cyk8 371-388 [wt] and Vim116-135[wt], $p < 0.0001$, with minimal cross reactivity to the wt peptides (Fig. 3D).

We previously showed responses to Modi-2 peptides in the CpG/MPLA adjuvant formulation were CD4-mediated. However, the SNAPvax formulation has been shown to enhance the potency of peptide-based vaccines that mainly induced CD8 T cells responses[21,24]. Therefore, we reinvestigated whether responses to Modi-2 SNAPvax formulation were CD4 or CD8 mediated. In Balb/c mice, responses to Aldo74-93[Hcit] were significantly reduced by anti-CD4 blocking antibody ($p = 0.0018$) and significantly, albeit partially, blocked by anti-CD8 blocking antibody ($p = 0.0032$) (Fig. 3E). Responses to Cyk8 371-388[Hcit] and Vim116-135[Hcit] were also significantly lost after blocking CD4 T cells, $p = 0.0041$ and $p = 0.0048$, respectively. Whereas there was no significant loss in these responses after blocking CD8 T cells in Balb/c (Fig. 3E). These results were consistent with results shown in the previous section where Modi-2 peptides were mixed with the adjuvants CpG/MPLA (Fig. 1G), confirming that IFNγ responses to Modi-2 SNAPvax formulations were also mediated by CD4 T cells. Immunogenicity analysis therefore suggests similar immune responses stimulated in mouse models from the large particulate peptide in CpG and MPLA formulation and the nanoparticle SNAPvax formulation.

## Homocitrulline-specific CD4 responses mediate tumour therapy in several mouse models

In the tumour environment MPO secreted by infiltrating MDSCs can mediate homocitrullination of proteins in the tumour microenvironment making homocitrullinated epitopes a promising target for tumour therapy. However, it is possible that not all lysines are naturally homocitrullinated and presented by MHCII to be recognised by CD4 T cells. We therefore aimed to investigate if the Hcit peptides in Modi2 vaccine are naturally presented by examining if the CD4 mediated IFNγ responses to Aldo74-93[Hcit], BiP562-579[Hcit], Cyk8 371-388[Hcit] and Vim116-135[Hcit] were sufficient to provide potent tumour therapy in vivo.

We first assessed the expression of Aldo A, Bip, Cyk8 and Vim native proteins in in vitro grown B16 HHDII iDP4, 4T1 and CT26 tumour cell lines by western blot. This assessment confirmed that Aldo A, Bip and Vim proteins were expressed in B16F1 HHDII iDP4, 4T1 and CT26 tumour cell lines. However, Cyk8 was only expressed in 4T1 and was not detected in in vitro grown CT26 and B16F1 HHDII iDP4 tumour cell lines. Py8119 tumour cells were used as a negative control for Cyk8 protein and a positive control for Vim protein. Py230 cells were used as a positive control for Cyk8 and a negative or low positive control for Vim. B16 HHDII iDP4 cells were used as a positive control for Aldo A. B16F1 cells treated with thapsigargin, an endoplasmic reticulum (ER) stress inducer that enhances the Bip expression[25], were used as a positive control for Bip protein (Fig. 4A, B). Raw images for western blots are shown in Supplementary Fig. 16.

As Modi-2 vaccine targets homocitrullinated proteins, we assessed the level of carbamylation (homocitrullination) in 4T1, CT26 and B16 HHDII tumours ex vivo. In the absence of homocitrullinated protein specific detection reagents a general anti-carbamylation antibody was used. Tumour cells isolated ex vivo from 4T1, CT26 and B16 HHDII tumours implanted subcutaneously were stained with anti-carbamylation antibody when reaching 10–15 mm in diameter. Representative staining is shown in Fig. 4Ci and average expression in Figure 4Cii. Gating strategy is shown in Supplementary Figure 7. Although homocitrullination/carbamylation is detected, this staining with the pan anti-carbamylation antibody does not detect if Aldo A, Bip, Cyk8 and Vim proteins expressed in tumour cells are specifically carbamylated.

Results mentioned above confirmed that 4T1, B16 and CT26 tumour models were suitable to assess the anti-tumour potency of the Modi-2 vaccine. Mice were therefore challenged with B16 HHDII iDP4 cells and vaccinated four days later with 4nmol of Modi-2 mixed with CpG/MPLA or 4nmol Modi-2 SNAPvax and compared to unimmunised or adjuvants alone. At the point of vaccination tumours were < 1 mm diameter. No difference was noted with adjuvants alone compared to unimmunised mice. Those vaccinated with 4nmol Modi-2 SNAPvax Histidine buffer formulation showed a significantly enhanced overall survival compared to unvaccinated mice ($p = 0.0009$) (Fig. 5A, B). Modi-2 CpG/MPLA formulation also showed 50% overall survival at day 50 which was significantly higher than the unvaccinated B16 HHDII iDP4-bearing mice $p = 0.0044$ (Fig. 5A, B). Similar findings were also seen in the CT26 tumour model with Modi-2 SNAPvax formulation. Adjuvants only had no impact on tumour therapy. The vaccination of CT26-bearing mice with 4nmol Modi-2 SNAPvax Tris buffer formulation or Modi-2 CpG/MPLA induced potent anti-tumour responses with 100% overall survival which was significantly higher than the unimmunised or adjuvant only immunised CT26-bearing mice, $p < 0.0001$ and $p = 0.0007$ respectively (Fig. 5C, D). The vaccination of 4T1-bearing mice with 4nmol of Modi-2 SNAPvax Histidine buffer formulation also showed significantly potent anti-tumour therapy with 70% overall survival respectively compared with the unvaccinated 4T1-bearing mice, $p = 0.0090$ respectively (Fig. 5E, F). Mice in all tumour therapy studies showed no clinical signs associated with autoimmunity and weights remained stable throughout the duration of the studies (Supplementary Fig. 8).

We further examined the tumour infiltrating lymphocytes (TILs) from tumours that developed in the Modi-2 SNAPvax vaccinated and unvaccinated 4T1-bearing mice. 4T1 tumours show a degree of cell death upon disaggregation but this is similar in both immunised and control animals and samples are gated to focus on the live TIL population (Supplementary Figure 9). The subsequent flow cytometry gating strategy is shown in Supplementary Figure 10. A representative staining example is shown in Fig. 5G. The analysis of tumours from Modi-2 SNAPvax immunised mice were those that failed therapy but despite this they showed evidence of a significant increase in infiltration of CD45+ cells into tumours. Within the CD45+ population there was a significant increase in CD4+ cells in vaccinated compared to control tumours (Fig. 5G). Supplementary Fig. 10 confirms that CD4+ cells within the CD45+ population are T cells. Modi-2 SNAPvax immunised mice also showed a significant increase in the expression of MHCII on both CD45+ and CD45- cells within tumours (Fig. 5G). The percentage of CD45-MHCII + in the tumours of unimmunised mice was significantly lower than seen in tumours from the vaccinated mice (Fig. 5G). Data across multiple mice is shown in Fig. 5H where a significant increase is demonstrated for CD4 T cell infiltration and MHCII expression. This data suggests the vaccine increases the leukocyte infiltration into tumours, particularly for CD4 T cells and that both lymphocytes and non-lymphocytes show an increase in MHCII reflecting a more proinflammatory environment but the analysis of tumours that failed therapy may be underestimating the effect of the Modi-2 vaccine. These results show that Modi-2 SNAPvax induced homocitrulline specific T cell responses that were sufficient to mediate tumour therapy in HLA-HHDII/DP4 and Balb/c mouse tumour models.
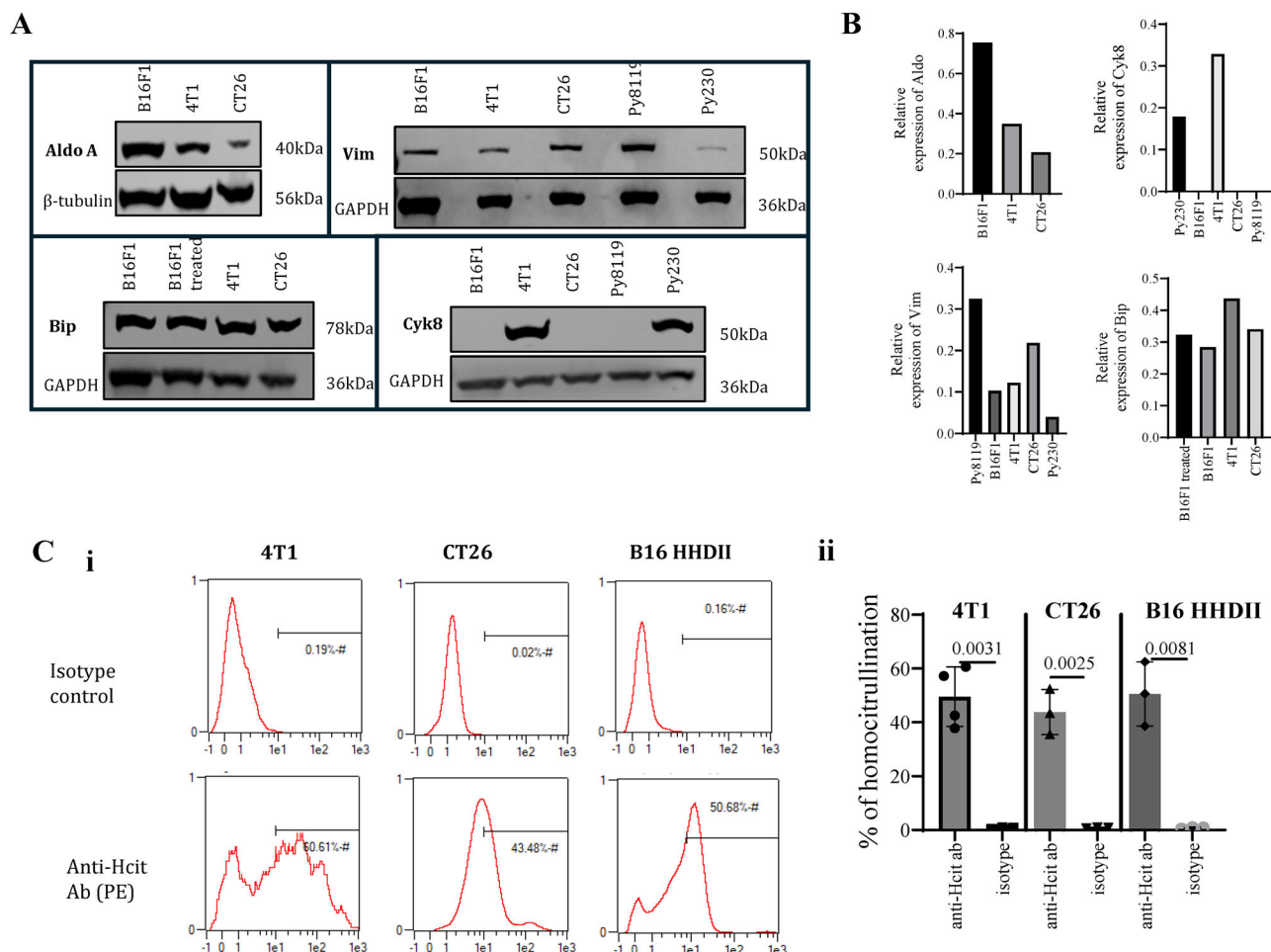
Fig. 4 | Murine tumours express Modi-2 target antigens and show evidence of carbamylation/homocitrullination. A, B The relative expression of Aldo, BiP, Cyk8 and Vim in different murine tumour cell lines measured by western blot. **C** The percentage of carbamylation in murine tumour cell lines ex vivo assessed by flow cytometry as representative staining histogram (i) and averages (ii). Anti-carbamyl lysine antibody staining is gated on live CD45- cells. Values show the percentage of gated cells staining positive. Mean of at least 3 independent samples, standard deviations and significant p values are shown.

Human tumours express Modi-2 target antigens and expression correlated with low overall survival rates

To screen which cancer patients may benefit from the Modi-2 vaccine, we assessed the expression of Modi-2 target proteins on tumour tissues derived from patients with breast, colorectal, lung and prostate cancer. breast, colorectal, lung and prostate TMAs were stained with specific antibodies for Aldo A, Bip, Cyk8 and Vim. Representative staining is shown in Fig. 6A. Analysis showed that the H-score of the staining for Aldo A, Bip and Cyk8 were significantly higher in colorectal cancer tissues compared with colorectal normal adjacent tissues, $p < 0.0001$, $p = 0.0017$, $p = 0.0005$ respectively (Fig. 6B). Our IHC results also showed that normal colorectal adjacent tissues showed significantly higher H-score of Vim staining than colorectal cancer tissues, $p < 0.0001$ (Fig. 6B). The breast cancer tissues also showed medium to high H-score staining to Aldo, Bip and Cyk8 proteins (Fig. 6C). However, the H-score staining of Vim was modest on breast cancer tissues. Unfortunately, breast TMAs did not include normal or normal adjacent tissues, therefore we could not compare the expression of proteins and the level of carbamylation between breast cancer and normal or normal adjacent tissues.

The IHC analysis also showed that the H-score of Aldo A, Bip and Cyk8 proteins was significantly higher on lung cancer tissues compared with lung normal adjacent tissues (Supplementary Fig. 11A). There was no significant difference in the H-score of Vim, carbamylation and MPO staining between lung cancer and normal adjacent tissues. Similar results observed on prostate TMAs (Supplementary Fig. 11B). These results confirm that Aldo A, Bip, Cyk8 and Vim were expressed with different intensity in several human tumours including breast, colorectal, lung and prostate. Representative staining images of low, moderate and high staining of Aldo A, Bip, Cyk8 and Vim on lung and prostate TMAs are shown in Supplementary Figure 12.

Unfortunately, survival data was not available for the TMAs stained in this study therefore we further investigated if the expression of these proteins are correlated with the overall survival in cancer patients from available data sets. In silico analysis of integrated proteo-transcriptomics dataset of breast cancer from Tang et al.[26] revealed that breast cancer patients with high expression of Aldo, Bip, Cyk8 and MPO, the enzyme responsible for carbamylation, had poor overall survival which was significantly decreased compared with patients who had low expression of those proteins, $p = 0.044$, $p = 0.0055$, $p = 0.0236$ and $p = 0.0040$, respectively (Supplementary Fig. 13A). In silico analysis of microarray gene expression colorectal cancer dataset (downloaded from www.kmplot.com) showed that colorectal cancer patients with high relative expression of Vim, Aldo, Cyk8 and MPO had poor overall survival which was significantly decreased compared with patients who had low relative expression of Vim, Aldo, Cyk8 and MPO, $p < 0.0001$, $p = 0.0008$, $p = 0.0152$ and $p = 0.0127$, respectively (Supplementary Fig. 13B).

In silico analysis of microarray gene expression lung cancer dataset (downloaded from www.kmplot.com) revealed that lung cancer patients with high relative RNA expression of Aldo A, BiP, Cyk8 and MPO were significantly associated with low overall survival rates in lung cancer
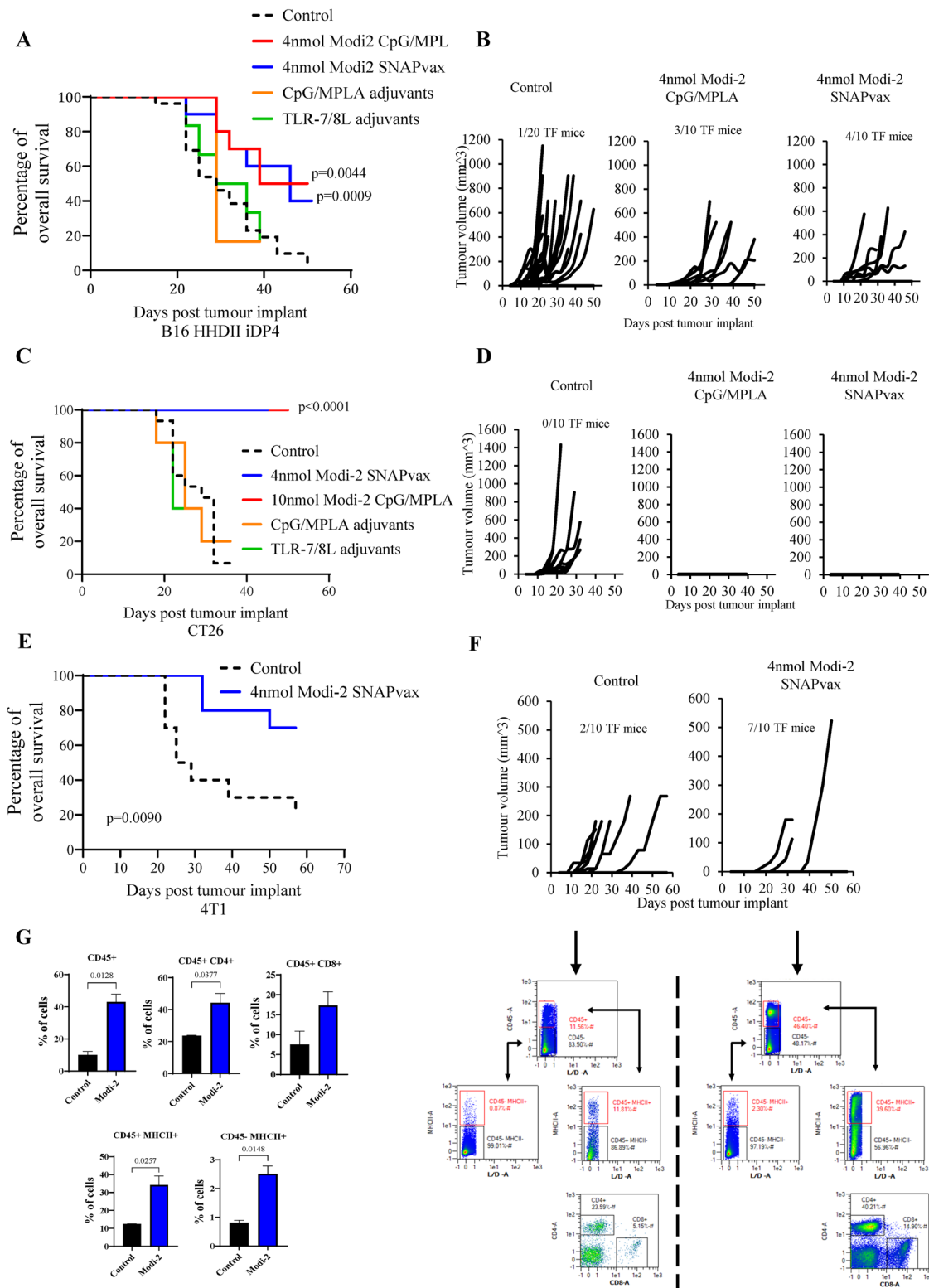
Fig. 5 | Modi-2 SNAPvax vaccination mediates tumour therapy. HHDII/DP4 transgenic (**A**, **B**) or Balb/c (**C–G**) mice were injected with 1 x 10^5 B16 HHDII/iDP4 (**A**, **B**), 1.75 x 10^4 CT26 (**C** and **D**) or 5 × 10^3 4T1 (**E–G**) tumour cells respectively on day 1 followed by immunisation with 4nmol Modi-2 peptides in CpG/MPLA or 4nmol of Modi-2 SNAPvax on days 4, 11 and 18 (**A**, **B**) or days 4, 8 and 11 (**C–G**). Overall survival (OS) and tumour growth monitored ($n \geq 5$). Numbers on tumour growth curves represent the number of tumour free (TF) mice out of the total. Survival analysed using LogRank test. (**G**), Tumours from 4T1 model disaggregated and stained ex vivo for CD45, CD8, CD4 infiltrate and MHCII expression. Representative tumour examples and histograms of averages ($n > 3$) with error bars of standard deviations are shown.
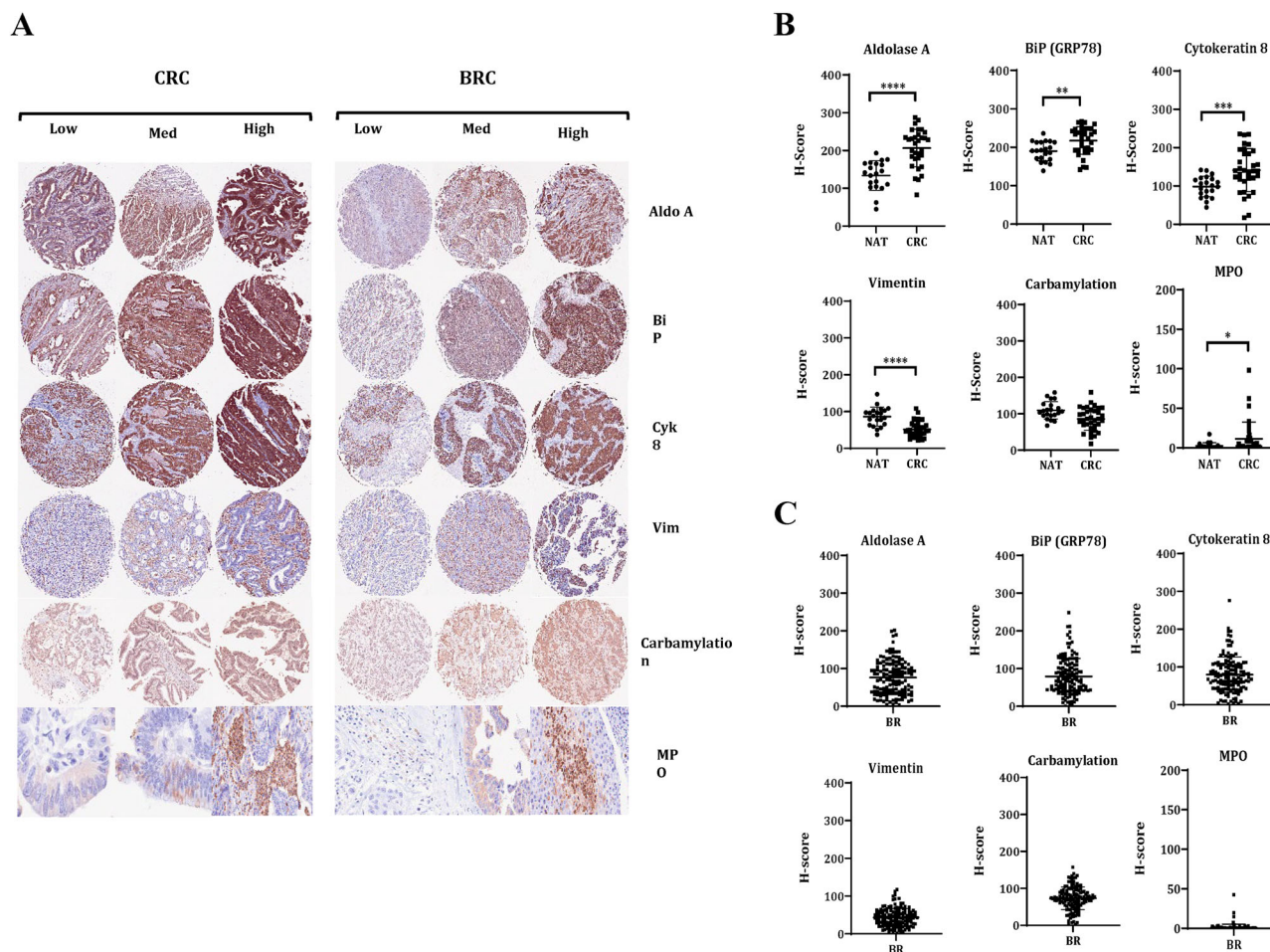
Fig. 6 | Human tumours express Modi-2 target antigens. Colorectal (CRC) and breast (BR) tumour microarrays stained by immunohistochemistry for vimentin, cytokeratin 8, aldolase A, BiP and MPO using antigen specific antibodies and homocitrullination using an anti-carbamyl antibody. **A** representative staining images of low, moderate and high staining. **B** Data shown as H-score for normal or normal adjacent tissue (NAT) compared to tumour tissue on the CRC TMAs. **C** Data shown as H-score for tumour tissue on the BR TMAs.

patients, $p < 0.0001$, $p = 0.0300$, $p < 0.0001$ and $p = 0.0004$, respectively (Supplementary Fig. 14). In silico analysis of RNAseq advanced prostate cancer dataset from Abida et al.[27] showed that patients with advanced prostate cancer with high relative expression of Cyk8 had poor overall survival which was significantly decreased compared with patients who had low expression of Cyk8, $p = 0.0079$ (Supplementary Fig. 15). This in silico data supports our IHC staining data and provides further evidence that expression of these proteins is altered in a variety of solid cancers and could be appropriate targets for immune therapy. Although there is no data on levels of carbamylation and overall survival, the enzyme MPO that is most often produced by a subset of MDSCs in tumours mediates carbamylation could be as an indication of carbamylation potential. The association of high MPO with lower survival and poorer prognosis suggests that carbamylation is also a candidate target for therapies.

Data presented in this study demonstrates the efficacy of the Modi-2 vaccine in murine tumour models and provides evidence that the Modi-2 vaccine has potential as tumour therapy to treat patients with solid tumours including breast, colorectal, lung and prostate that express Aldo A, Bip, Cyk8, Vim and MPO.

Discussion

We have previously demonstrated that targeting homocitrullinated (Hcit) peptides induces potent anti-tumour immune responses in animal models[5,11]. Here, we presented the potential of a combination Modi-2 cancer vaccine as a promising therapy for solid tumours. Modi-2 vaccine is designed to target specific peptides including Aldo74-93[Hcit], BiP562-579[Hcit], Cyk8 371-388[Hcit] and Vim116-135[Hcit]. These peptides are derived from four abundant proteins; aldolase A, BiP, cytokeratin 8 and vimentin, which are found to be highly upregulated in many solid tumours[28].

Homocitrullination is a post-translational modification by which lysine residues are converted to homocitrulline, leading to generation of neoepitopes that may bypass self-tolerance. Homocitrullination is induced by cumulative levels of cyanate which results from the breakdown of urea. This also can be mediated through the action of MPO which is secreted by several immune cells including neutrophils, macrophages and MDSCs within inflammatory environments[9]. The levels of MPO have been assessed in solid tumours. The level of MPO is found to be significantly secreted by infiltrating macrophages and neutrophils within breast cancer tissues[29]. The high levels of MPO are found to correlated with a poor prognosis and low overall survival rates in patients with colorectal cancer (CRC)[30]. The enzymatic activity of MPO is found to be indispensable for tumour initiation and progression in Balb/cByJ mouse lung cancer tumour model. The inhibition of MPO activity could reduce lung tumour burden by 50%[31]. In our *in-silico* analyse we have also shown that the high levels of MPO are correlated with poor overall survival in patients with breast cancer, CRC and lung cancer. These findings were also associated with our IHC staining of anti-carbamylation antibody on breast, CRC, lung, and prostate TMAs. Homocitrullination is a known PTM in autoimmune disease and therefore there is a possibility of stimulating autoimmune toxicities and

should be monitored for in any future clinical study. However, there has been no indication of toxicity indicative of autoimmunity in our murine models[5,11].

Our data have demonstrated that despite AldoA, Bip, Cyk8 and Vim being self-proteins, vaccination with Modi-2 Hcit peptides induced strong immune responses in two different mouse strains; HLA-HHDII/DP4 and Balb/c. Responses to Modi-2 Hcit peptides are mediated by CD4 T cells and are homocitrulline-specific with minimal cross reactivity to the wild type (wt) peptides. These findings are also consistent with our previous works which also showed that two of Modi-2 peptides (Cyk8 371-388[Hcit] and Vim116-135[Hcit]) induced strong immune responses in HLA-HHDII/DR1 mice[5,11]. These findings provide further evidence that responses to Modi-2 Hcit peptides may act through several HLA alleles[11]. We have demonstrated the presence of a responding CD4 repertoire to the homocitrullinated peptides in healthy humans in our previous data[5,11]. Donors possessed a range of HLA alleles suggesting more than one HLA type can present these peptides. However, we have yet to confirm the HLA restriction of Modi-2 Hcit responses in a larger cohort of healthy donors. This data suggests that CD4 responses to these modified self-antigens are not deleted or tolerised.

Tumour cells can express MHC class II molecules but most often these are absent or at low level until expression is upregulated through inflammatory pathways. Tumour therapy was observed against models where MHC class II is inducible by IFNγ and evidence of significantly increased MHCII expression was seen in the tumour microenvironment in combination with increased CD4 T cell infiltrate after vaccination. Therefore, the CD4 T cell response can exert both direct and indirect effects upon the tumour to promote inflammation and MHCII upregulation. Indeed, in our previous work CD4 T cells were shown to be essential for Hcit peptide vaccine mediated tumour therapy[5]. An increase in immune infiltrate is associated with increased immune pressure that can drive tumour escape. It is well-known that cancer immune escape is mainly mediated by mechanisms including antigen loss and the loss of MHC class I and II expression[32,33]. Therefore targeting several epitopes derived from different antigens simultaneously within a vaccine that induces immune responses through several MHC class II alleles helps to overcome tumour immune escape via antigen and HLA loss[34]. In addition, the targeting of longer epitope sequences does not exclude the possibility of also stimulating CD8 T cell responses and we have previously shown that CD8 T cell responses can be induced to homocitrullinated peptides[35]. However, CD8 T cell responses were not observed to the peptides restricted through the HLA alleles tested in this study and CD4 T cell responses were sufficient to mediate tumour therapy.

The efficacy of therapeutic peptide-based vaccines for inducing potent immune responses is based on the selection of an effective adjuvant and delivery system[36]. Our data have shown that the formulation of Modi-2 Hcit peptides mixed with the CpG/MPLA adjuvants induced potent anti-tumour immune responses in the aggressive murine B16 tumour model. However, our data have also confirmed that the Modi-2 CpG/MPLA formulation showed aggregation and low solubility in aqueous solvents, which is likely not suitable for manufacturing at commercial scale for clinical use. It is well-known that immunogenic peptides are enriched for hydrophobic and aromatic amino acids which reduce their solubility in aqueous buffers[37]. These factors make manufacturing peptide-based vaccines to clinical GMP grade more challenging. In addition, it has been demonstrated that the adjuvant effects of TLR ligands can be enhanced and stronger immune responses stimulated if peptide and adjuvant are codelivered to the same APC[19,20].

Here we demonstrate the use of SNAPvax technology which makes use of the hydrophobicity of TLR7/8 adjuvant and peptides to improve both manufacturability (through improved solubility of peptide antigens) and maintain immune responses of the Modi-2 vaccine. The Modi-2 SNAPvax formulations provided particles of uniform size (~20 nm) known to increase activation of and uptake by APCs[21,22] and – through covalent linkage of the peptide antigens directly to TLR-7/8 ligand – enable both adjuvant and all four peptides to be delivered to the same APC. The potential for uptake and presentation of multiple peptides by the same APC may lead to immune competition either from competition for MHC binding or for T cell access to the APC. This is known to occur for CD8 T cell responses, however, in our murine in vivo studies we did not observe any immune dominance effect on the stimulation of CD4 T cell responses. The delivery of peptide and adjuvant as a nanoparticle formulation in the SNAPvax technology has previously been shown to increase persistence of the vaccine at the dose site and draining lymph nodes as well as the uptake by APC subsets and increase in associated cytokines in vaccine draining lymph nodes[21,22]. Although the biodistribution of the specific Modi2 SNAPvax formulation has not been demonstrated in this study, prior studies suggest that the APC uptake and stimulating ability is equally effective with different immunogenic peptide components[21]. Though the SNAPvax technology has been demonstrated to be effective for stimulation of CD8 T cell responses, particularly to hydrophobic peptides that are difficult to formulate, our results build on prior findings showing that the SNAPvax technology also to be effective for inducing CD4 T cell responses associated with efficacy in murine tumour models. Modi-2 SNAPvax formulations induced potent anti-tumour responses with 40%, 100% and 70% overall survival rates in three aggressive tumour models, B16 HHDII iDP4, CT26 and 4T1, respectively. Our data have also demonstrated that Modi-2 SNAPvax formulations dramatically enhanced infiltration of TILs in particular of total CD4 T cells, and both CD45+ immune cells and CD45- non-immune cells showed a significant increase in MHC class II expression within tumours suggesting the CD4 responses stimulated by vaccination mediate an alteration of the tumour microenvironment. It would certainly be interesting in future studies to confirm the presence of vaccine specific CD4 T cells in the tumour microenvironment. Reports for the stimulation of CD8 T cell responses using the SNAPvax technology suggest systemic localisation and more sustained responses when delivered via intravenous route rather than via a subcutaneous route but it remains to be determined if this observation of sustained responses is also true for CD4 responses[23]. Although we have not tested the potency of Modi-2 SNAPvax formulations in tumour models for prostate and lung cancer, our in silico analyses suggest that the Modi-2 vaccine may also be beneficial for these cancer types.

Cancer vaccines have begun to show efficacy in preventing recurrence post resection[8,38]. This study presents the efficacy of a Modi-2 SNAPvax formulation as a promising therapeutic cancer vaccine to treat several solid tumours. The nature of homocitrullination in the tumour environment suggests a role for Modi-2 in patients with existing tumours but the majority of patients with existing solid and untreatable tumours will likely have established tumour intrinsic mechanisms of immune evasion. These patients would therefore likely require combination with other interventions such as checkpoint blockade therapies to help overcome the immune suppression associated existing tumour mass in combination with vaccination to generate de novo tumour specific immune responses.

Methods
Study design
The aim of this study was to assess the efficacy of Modi-2 vaccine to induce potent tumour therapy in pre-clinical mouse models that may mimic solid human cancers. Also to assess the potential of the SNAPvax formulation to improve vaccine manufacturability to GMP clinical grade. To achieve this, we used age-specific murine in vivo and in vitro models. Sample size and age criteria were chosen empirically based on the results of previous studies and power calculations. Animal experiments were performed under the UK Home Office approved project license (PP2706800) and with ethical approval from Nottingham Trent University and University of Nottingham Ethical review boards. Mouse experiments aimed to include 3 mice per group for immune response analysis studies and 10 mice per group for in vivo tumour studies. Data was combined from at least two or more independent experiments. Mice were randomly assigned to different treatment groups and for the tumour inoculation but were not blinded to the investigators. No mice were excluded from the experiments. Mice were terminated when conditions approached the limits specified on the project

licence. Human tissue microarrays (TMA) slides were purchased from Insight Biotechnology, processed and archived according to the Human Tissue Authority (HTA) license (Scancell Ltd #12768).

Peptides and adjuvants

IEDB predicted binding scores were described previously[11]. Sequences of peptides used in this study are listed in Supplementary Table 1. Peptides were synthesised at > 90% purity (Genscript and JPT), stored lyophilised at −80 °C and then reconstituted to the appropriate concentration in 20% DMSO/PBS or 20%DMSO/distilled H$_2$O on day of use. Adjuvants TLR9 agonist CpG ODN 1826 (In vivogen) and TLR4 agonist Monophosphoryl Lipid A (MPLA) (InvivoGen) were used at 5 μg dose unless stated otherwise.

SNAPvax

SNAPvax formulations of the Modi-2 vaccine were prepared as previously described by Lynn et al.[21] In brief, amphiphilic peptides capable of undergoing nanoparticle self-assembly were prepared in two steps. Peptide antigen fragments consisting of a charge-modifying group linked to the N-terminus of each of the 4 homocitrullinated peptide antigens were prepared using solid-phase peptide synthesis performed by GenScript (Piscataway, NJ, USA). Peptide antigen fragments were then covalently linked to hydrophobic oligopeptides ("hydrophobic blocks") comprising TLR-7/8 ligands using a copper-free strain-promoted azide-alkyne cycloaddition click chemistry reaction to yield amphiphilic peptide antigen conjugates. Nanoparticle formulations were produced by addition of the indicated aqueous buffer and the resulting solutions were used for vaccination without any further medication or preparation.

Formulation characterisation

Particle size distribution profile (particle size & polydispersity index) of Modi-2 formulations was analysed by dynamic light scattering (DLS) technique using a Zetasizer ultra red instrument (Malvern Panalytical, Malvern, UK). Same instrument was used to determine zeta potential of formulations by laser Doppler velocimetry (LDV) technique. Particle morphology was analysed by FEI Tecnai 12 Transmission electron microscope fitted with Gatan OneView CMOS camera. The %Recovery of Modi-2 peptides via a 0.2 μm PES filter media was determined by UV-Visible spectrophotometry using UV5Nano instrument (Mettler Toledo, Leicester, UK) at wavelength of 325 nm. The identification of Modi-2 peptides was confirmed by an UPLC method using the ACQUITY H-Class Plus UPLC system equipped with a photo diode array (PDA) detector and quadrupole mass detector (Waters, Massachusetts, USA).

Animals and cell lines

Animal experiments were carried out with ethical approval from University of Nottingham and Nottingham Trent University ethical review boards and under a Home Office approved project license (PP2706800). HLA-HHDII/DP4 (HLA-A2.1 + / + HLADP4 + /+ hCD4 + /+, EM:02221, European Mouse Mutant Archive) transgenic mice knocked out for murine MHC-I and II and expressing chimeric HLA-A2 (HHDII), human HLA-DP4 and human CD4 or Balb/c mice (Charles River) aged 6–12 weeks were used.

The murine melanoma B16F1 cell line (ATCC-CRL-6323) obtained from ATCC was knocked out for murine MHCI and II and transfected with HHDII in combination with IFNg inducible HLA-DP4 (iDP4) using plasmids as described previously[39]. Cells were cultured in RPMI medium 1640 with L-glutamine (2 mmol/L), 10% FCS and appropriate antibiotics to maintain plasmids. The murine breast cancer 4T1 cell line (ATCC-CRL-2539) and colon cancer CT26.WT cell line (ATCC-CRL-2638) obtained from ATCC were cultured in RPMI medium 1640 supplemented with 10% FCS. Cell lines utilized were mycoplasma free, authenticated by suppliers (STR profiling), and used within ten passages.

Immunisation protocol

Mice were vaccinated with Modi-2 vaccine comprising 10 μg (4 ηmol) or 25 μg (10 ηmol) each of the four homocitrullinated peptides mixed with 5 μg

each of CpG and MPLA adjuvants or as SNAPvax formulations. Modi-2 SNAPvax were formulated in Histidine (50 mM, pH 6.5), Tris (50 mM, pH 7.4) or PBS (pH 7.4). Peptides were injected intradermally (i.d.) or intramuscularly (i.m.) in 50 μl volume on days 1, 8 and 15. No anaesthesia was used for injections. Responses were screened on day 21 after euthanasia by cervical dislocation.

For anti-tumour experiments, mice were implanted s.c. with tumour cells three days prior to immunisation with Modi-2 vaccine. Implant doses were 1×10^5/mouse for B16 HHDII iDP4 cell line, 5×10^3/mouse for 4T1 cells and 1.75×10^4/mouse for CT26 cells. Immunisation (as described above) was on days 4, 11 and 18 for the B16 HHDII iDP4 tumour model and it was on days 4, 8 and 11 for the 4T1 and CT26 tumour models. Tumour growth was monitored twice weekly, and mice were euthanized by cervical dislocation once tumours approach the license limit of 15 mm in diameter. Tumour growth in mice was analysed by measuring the tumour size with callipers (length and width). Volume was estimated by the formula (volume = (π/6) x (width x length^2).

Ex vivo ELISpot assay

Elispot assays were performed using murine IFNγ capture and detection reagents according to the manufacturer's instructions (Mabtech). In brief, the IFNγ specific antibody were coated onto wells of 96-well Immobilin-P plate. Synthetic peptides at 10 μg/ml diluted in culture media (RPMI medium 1640 (GIBCO/BRL) supplemented with 10% FCS (Sigma), 2 mM L-glutamine (Sigma) and sodium bicarbonate buffered with additional 20 mM HEPES (Sigma) and 50 μM 2-mercaptoethanol (Thermofisher)) and 5×10^5 per well splenocytes were added to the wells of the plate in quadruplicate and plates incubated for 40 h at 37 °C with 5% CO$_2$. Cells with culture media only were added as negative control and 5 μg/ml Lipopolysaccharide (LPS, Sigma) was used as a positive control. 20 mg/ml anti-CD8 (2.43, Cat #: BP0061, InVivoPlus +), anti-CD4 (GK1.5, Cat #: BP0003-1, InVivoPlus +) or anti-human CD4 (RPA-TA, Invitrogen, 16-0049-85) antibodies were added to appropriate wells for blocking studies. After incubation, captured IFNγ was detected by biotinylated specific IFNγ antibody and developed with a streptavidin alkaline phosphatase and chromogenic substrate. Spots were analyzed and counted using an automated plate reader (Cellular Technologies Ltd).

Western blot

B16F1, 4T1, CT26, Py8119, and Py230 cell lines were lysed with RIPA buffer supplemented with 1% of protease and phosphatase inhibitors cocktail (Thermo Scientific™, 78440). 20 μg reduced protein samples were loaded on a precast polyacrylamide gel (Invitrogen, NW04125BOX) and run at 130 V for 50 min followed by a transfer to nitrocellulose membranes at 30 V for 90 min. After blocking with 5% non-fat milk the membrane was incubated with relevant antibodies (Supplementary Table 2) overnight at 4 °C on a roller. Following 3× wash the membrane was incubated with secondary antibodies (Supplementary Table 2) for 60 min in the dark at room temperature. The membranes were then washed and analysed using LI-COR ODYSSEY scanner.

Immunohistochemistry

List of materials and antibodies used in the IHC can be found in Supplementary Tables 3 and 4. Novolink polymer detection system (RE7150-K, Leica BIOSYSTEMS) was followed during IHC-P staining procedure which was carried out at room temperature. Slides were dewaxed, rehydrated and immersed in fresh xylene followed by fresh IMS (industrial methylated spirit) and water. Heated-induced antigen/epitope retrieval was performed in 1x citrate buffer pH 6 (Antigen Retrieval Buffer (100x Citrate Buffer pH 6.0), ab93678, Abcam). Slides were then cooled and rinsed, and peroxidase block solution was applied followed by 10% normal goat serum and protein block. Antibody diluent solution was prepared by mixing 1 part of blocker casein in PBS solution (BlockerTM Casein in PBS, 37528, Thermo Scientific) and 9 parts of BOND primary antibody diluent (AR9352, Leica Biosystems). Primary antibodies at different dilution/concentration in antibody

diluent solution were applied onto relevant slides. For detection Novolink polymer solution was applied onto slides followed by rinse and wash with PBS-Tween. Novolink DAB/substrate working solution (1:20 dilution, DAB chromogen in DAB substrate buffer) was applied onto slides and then slides were then rinsed and washed with PBS-Tween. Haematoxylin solution (Mayer's, Modified, ab220365, Abcam) was applied followed by washing under slow-running tap water. Slides were then dehydrated in a series of three fresh IMS baths and cleared in a series of two fresh xylene baths. Slides were then mounted with coverslips (Thickness 1 (20 x 40 mm), 2975-244, Corning) using DPX mounting medium (DPX Mountant for histology, BCCD8334, Sigma).

High-resolution digital scans of microscopic slides were acquired using the NanoZoomer (Hamamatsu) whole slide scanner. Biomarker scoring of the tissue was performed using QuPath software version 3.0. To identify tissue cores, QuPath's automated Tissue Microarray (TMA) dearrayer was used in batch mode for all slides within each project. The resulting TMA grid was manually inspected and corrected as necessary by adjusting core positions or removing cores placed in artifact-filled areas. To enhance stain separation, stain vector estimation and background correction were applied to each immunohistochemistry (IHC) analysis project using QuPath's Estimate stain vectors command. This involved identifying stain vectors within a typical region that had a background area, as well as strong hematoxylin and DAB staining. The generated stain vectors were then applied to all images in the project. After the TMA pre-processing steps, positive cell detection was performed using QuPath's command. Cells were categorised as positive or negative based on three intensity thresholds applied to the DAB optical density within the entire cell area. The summary scores were calculated based on the total number of cells detected per core and the number of cells classified as negative, weakly, moderately, and strongly stained cells within the total cell population. A H-score was assigned to each tissue core, ranging from 0 (all negatively stained) to 300 (all strongly positively stained).

Staining of tumours in vitro and ex vivo

Tumours were mechanically disaggregated in 10 ml of RPMI medium. Clumps were allowed to settle out. Samples of tumour cell suspension were taken for staining. Cells were stained with live/dead stain (LIVE/DEAD™ Fixable Violet Dead Cell Stain Kit, Invitrogen, L34955). Fc receptors were blocked using FcR blocking reagent (mouse, Miltenyi, 130-092-575. Cells were stained with anti-mouse CD45, CD4, CD8, MHCII antibodies and anti-carbamylation antibody. (Supplementary Table 5).

In silico data analysis

Lung and colorectal cancer microarray gene expression (mRNA chip) normalised datasets were downloaded from www.kmplot.com. Relative mRNA expressions of Aldo, Bip, Cyk8, Vim and MPO were stratified into high and low based on the median of expressions values. Breast cancer proteotranscriptomics dataset was obtained from Tang et al.[26]. Normalised data were downloaded from www.kmplot.com. Relative protein expressions of of Aldo, Bip, Cyk8, Vim and MPO were stratified into high and low based on the median of expressions values. Advanced prostate cancer RNAseq dataset was originally obtained from Abida et al.[27]. Normalised data were downloaded from www.cbioportal.com.

Statistical analysis

Statistical analysis was performed using GraphPad Prism software version 10. Comparative analysis of the ELISpot results was performed by applying paired or unpaired ANOVA or Student t-test as appropriate with P-values calculated accordingly. Comparison of tumour survival was assessed by log-rank test. $P < 0.05$ values were considered statistically significant.

Data availability

The raw data supporting the conclusions of this article will be made available by the authors, without undue reservation. All data are available in the main text or the supplementary materials.

References

1. Rein, T. Post-translational modifications and stress adaptation: the paradigm of FKBP51. *Biochem. Soc. Trans.* **48**, 441–449 (2020).
2. Ting, Y. T. et al. The interplay between citrullination and HLA-DRB1 polymorphism in shaping peptide binding hierarchies in rheumatoid arthritis. *J. Biol. Chem.* **293**, 3236–3251 (2018).
3. Mydel, P. et al. Carbamylation-dependent activation of T cells: a novel mechanism in the pathogenesis of autoimmune arthritis. *J. Immunol.* **184**, 6882–6890 (2010).
4. Burska, A. N. et al. Autoantibodies to posttranslational modifications in rheumatoid arthritis. *Mediators Inflamm.* **2014**, 492873 (2014).
5. Cook, K. W. et al. Homocitrullination of lysine residues mediated by myeloid-derived suppressor cells in the tumor environment is a target for cancer immunotherapy. *J. Immunother. Cancer* **9**, e001910 (2021).
6. Hu, Z. et al. Personal neoantigen vaccines induce persistent memory T cell responses and epitope spreading in patients with melanoma. *Nat. Med.* **27**, 515–525 (2021).
7. Ott, P. A. et al. A Phase Ib Trial of Personalized Neoantigen Therapy Plus Anti-PD-1 in Patients with Advanced Melanoma, Non-small Cell Lung Cancer, or Bladder Cancer. *Cell* **183**, 347–362.e324 (2020).
8. Rojas, L. A. et al. Personalized RNA neoantigen vaccines stimulate T cells in pancreatic cancer. *Nature* **618**, 144–150 (2023).
9. Shah, S. et al. What do cancer-specific T cells 'see'? *Discov. Immunol.* **2**, kyac011 (2023).
10. Curran, A. M. et al. Citrullination modulates antigen processing and presentation by revealing cryptic epitopes in rheumatoid arthritis. *Nat. Commun.* **14**, 1061 (2023).
11. Cook, K. et al. Vaccine Can Induce CD4-Mediated Responses to Homocitrullinated Peptides via Multiple HLA-Types and Confer Anti-Tumor Immunity. *Front Immunol.* **13**, 873947 (2022).
12. Kreiter, S. et al. Mutant MHC class II epitopes drive therapeutic immune responses to cancer. *Nature* **520**, 692–696 (2015).
13. Alspach, E. et al. MHC-II neoantigens shape tumour immunity and response to immunotherapy. *Nature* **574**, 696–701 (2019).
14. Quezada, S. A. & Peggs, K. S. Tumor-reactive CD4+ T cells: plasticity beyond helper and regulatory activities. *Immunotherapy* **3**, 915–917 (2011).
15. Xie, Y. et al. Naive tumor-specific CD4(+) T cells differentiated in vivo eradicate established melanoma. *J. Exp. Med.* **207**, 651–667 (2010).
16. Ossendorp, F., Mengede, E., Camps, M., Filius, R. & Melief, C. J. Specific T helper cell requirement for optimal induction of cytotoxic T lymphocytes against major histocompatibility complex class II negative tumors. *J. Exp. Med.* **187**, 693–702 (1998).
17. Yang, Y., Huang, C. T., Huang, X. & Pardoll, D. M. Persistent Toll-like receptor signals are required for reversal of regulatory T cell-mediated CD8 tolerance. *Nat. Immunol.* **5**, 508–515 (2004).
18. Zom, G. G. et al. TLR2 ligand-synthetic long peptide conjugates effectively stimulate tumor-draining lymph node T cells of cervical cancer patients. *Oncotarget* **7**, 67087–67100 (2016).
19. Zom, G. G. et al. Efficient induction of antitumor immunity by synthetic toll-like receptor ligand-peptide conjugates. *Cancer Immunol. Res.* **2**, 756–764 (2014).
20. Brentville, V. A. et al. Combination vaccine based on citrullinated vimentin and enolase peptides induces potent CD4-mediated anti-tumor responses. *J. Immunother. Cancer* **8**, e000560 (2020).
21. Lynn, G. M. et al. Peptide-TLR-7/8a conjugate vaccines chemically programmed for nanoparticle self-assembly enhance CD8 T-cell immunity to tumor antigens. *Nat. Biotechnol.* **38**, 320–332 (2020).
22. Lynn, G. M. et al. In vivo characterization of the physicochemical properties of polymer-linked TLR agonists that enhance vaccine immunogenicity. *Nat. Biotechnol.* **33**, 1201–1210 (2015).

23. Baharom, F. et al. Systemic vaccination induces CD8(+) T cells and remodels the tumor microenvironment. *Cell* **185**, 4317–4332 e4315 (2022).

24. Baharom, F. et al. Intravenous nanoparticle vaccination generates stem-like TCF1+ neoantigen-specific CD8+ T cells. *Nat. Immunol.* **22**, 41–52 (2021).

25. Chen, L. Y., Chiang, A. S., Hung, J. J., Hung, H. I. & Lai, Y. K. Thapsigargin-induced grp78 expression is mediated by the increase of cytosolic free calcium in 9L rat brain tumor cells. *J. Cell. Biochem.* **78**, 404–416 (2000).

26. Tang, W. et al. Integrated proteotranscriptomics of breast cancer reveals globally increased protein-mRNA concordance associated with subtypes and survival. *Genome Med.* **10**, 1–14 (2018).

27. Abida, W. et al. Genomic correlates of clinical outcome in advanced prostate cancer. *Proc. Natl. Acad. Sci.* **116**, 11428–11436 (2019).

28. Ye, Z. et al. Prognostic values of vimentin expression and its clinicopathological significance in non-small cell lung cancer: a meta-analysis of observational studies with 4118 cases. *PLoS One* **11**, e0163162 (2016).

29. Ambrosone, C. B. et al. Myeloperoxidase genotypes and enhanced efficacy of chemotherapy for early-stage breast cancer in SWOG-8897. *J. Clin. Oncol.* **27**, 4973 (2009).

30. Weng, M. et al. Increased MPO in colorectal cancer is associated with high peripheral neutrophil counts and a poor prognosis: A TCGA with propensity score-matched analysis. *Front. Oncol.* **12**, 940706 (2022).

31. Rymaszewski, A. L. et al. The role of neutrophil myeloperoxidase in models of lung tumor development. *Cancers (Basel)* **6**, 1111–1127 (2014).

32. Olson, B. M. & McNeel, D. G. Antigen loss and tumor-mediated immunosuppression facilitate tumor recurrence. *Expert Rev. Vaccines* **11**, 1315–1317 (2012).

33. Warabi, M., Kitagawa, M. & Hirokawa, K. Loss of MHC class II expression is associated with a decrease of tumor-infiltrating T cells and an increase of metastatic potential of colorectal cancer: immunohistological and histopathological analyses as compared with normal colonic mucosa and adenomas. *Pathol. Res Pr.* **196**, 807–815 (2000).

34. Abd-Aziz, N. & Poh, C. L. Development of peptide-based vaccines for cancer. *J. Oncol.* **2022**, 9749363 (2022).

35. Shah, S. et al. Vaccination with post-translational modified, homocitrullinated peptides induces CD8 T-cell responses that mediate antitumor immunity. *J. Immunother. Cancer* **11**, e006966 (2023).

36. Khong, H. & Overwijk, W. W. Adjuvants for peptide-based cancer vaccines. *J. Immunother. Cancer* **4**, 1–11 (2016).

37. Riley, T. P. et al. Structure based prediction of neoantigen immunogenicity. *Front. Immunol.* **10**, 2047 (2019).

38. Weber, J. S. et al. Individualised neoantigen therapy mRNA-4157 (V940) plus pembrolizumab versus pembrolizumab monotherapy in resected melanoma (KEYNOTE-942): a randomised, phase 2b study. *Lancet* **403**, 632–644 (2024).

39. Brentville, V. A. et al. T cell repertoire to citrullinated self-peptides in healthy humans is not confined to the HLA-DR SE alleles; Targeting of citrullinated self-peptides presented by HLA-DP4 for tumour therapy. *Oncoimmunology* **8**, e1576490 (2019).

Author contributions

Conceptualization: L.G.D., V.A.B.; Methodology: A.A.A., K.W.C., P.S., A.S., Y.Z., V.L.C., O.J.M., R.H.C., N.U., P.R., A.P., G.M.L.; Investigation: A.A.A., K.W.C., P.S., A.S., A.W., P.R., N.U., A.P.; Visualization: A.A.A., G.M.L., S.E.A., V.A.B.; Supervision: V.A.B.; Writing – original draft: A.A.A., V.A.B.; Writing – review & editing: A.A.A., G.M.L., L.G.D., V.A.B.

Additional information

Supplementary information The online version contains supplementary material available at https://doi.org/10.1038/s41541-024-01029-1.

Correspondence and requests for materials should be addressed to Lindy G. Durrant.

Reprints and permissions information is available at http://www.nature.com/reprints

Publisher's note Springer Nature remains neutral with regard to jurisdictional claims in published maps and institutional affiliations.